Nuorivaara, Ted; Serna-Guerrero, Rodrigo

Unlocking the potential of sustainable chemicals in mineral processing : Improving sphalerite flotation using amphiphilic cellulose and frother mixtures

Unlocking the potential of sustainable chemicals in mineral processing: Improving sphalerite flotation using amphiphilic cellulose and frother mixtures
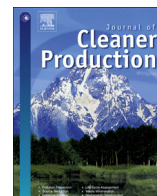
Ted Nuorivaara , Rodrigo Serna-Guerrero [*]

Department of Chemical and Metallurgical Engineering, School of Chemical Engineering, Aalto University, PO Box 16200, FI-00076, Aalto, Finland

ABSTRACT

The transition towards cleaner production of primary minerals demands technologies that improve productivity while lowering their environmental impact. The present study explores a novel approach to support this transition by partially substituting a commercial froth stabilization reagent in mineral froth flotation (DowFroth200) with an amphiphilic cellulose derivative (namely, hydroxypropyl methyl cellulose) that is nontoxic, biodegradable and can be produced from sustainable sources. The performance of the cellulose-frother mixture is explored using sphalerite as case study.

In the first place, the interaction between the two frother molecules was studied from the perspective of two-phase foam characteristics. The use of the polymer-surfactant (PS) mixture studied reported an increased foam stability and small bubble sizes, attributed to a combination of liquid film drainage prevention and steric effects of cellulose macromolecules. As a result, when used as frothers in the flotation of sphalerite, the PS-mixture exhibited a robust behavior resulting in advantages such as: i) improved separation efficiencies; ii) consistent recovery values, even under highly alkaline pH, iii) maintaining high recoveries when the collector dosage was reduced down to 25% of typical values used in the industry; and iv) faster flotation kinetics. The results obtained aim to demonstrate that properly designed green chemical systems can have a positive impact in the mining sector.

© 2020 The Authors. Published by Elsevier Ltd. This is an open access article under the CC BY-NC-ND license (http://creativecommons.org/licenses/by-nc-nd/4.0/).

1. Introduction

The need for practices with low environmental impact in the field of mineral processing is becoming evident, fueled by the awareness of the public and the commitments of governments to reduce hazardous emissions (Aznar-Sánchez et al., 2019). As a consequence, the mining industry is facing the challenge to develop processes that will ensure its continuous social licence to operate. According to Nagaraj and Farinato (2016), for example, the evolution of mineral froth flotation is currently ongoing a so-called "emerging period", where researchers should focus their efforts into finding solutions that improve the resource efficiency of the flotation process to match the strict environmental regulations of the future. Not surprisingly, concepts like "circular economy" have captured the attention of academics and industrial sectors dedicated to the production of raw materials alike (Kinnunen and Kaksonen, 2019; van Schalkwyk et al., 2018). The popularity of circular economy is based on its premise of value preservation throughout the life cycle of materials, thus avoiding waste generation and the unnecessary consumption of natural resources (Stahel, 2016; Velázquez Martínez et al., 2019). Interestingly, an approach that remains largely unexplored is the use of green chemistry to support mineral processing operations, although some recent studies have already explored alternatives with an aim to improve the sustainability of the flotation process (Huang et al., 2018, 2019 Peçanha et al., 2019). According to its definition, green chemicals should be less hazardous, (bio)degradable, or sustainably produced alternatives to State-of-the-Art technologies (Keijer et al., 2019). One can find macromolecules, which fulfill several of the aforementioned characteristics, among the wide variety of cellulose derivatives, for example. Admittedly, green chemistry in the mineral processing field will likely be implemented only when comparative advantages over currently used reagents are demonstrated.

With the aim to support the sustainable development of mining operations, the present work proposes a novel approach on the use

* Corresponding author.
E-mail address: rodrigo.serna@aalto.fi (R. Serna-Guerrero).

of cellulose derivatives to support mineral froth flotation operations. In this exploratory work, a formulation based on the partial substitution of commercial froth stabilization agents (a.k.a., *frother*) with hydroxypropyl methyl cellulose (HPMC) is proposed. The result is a mixed polymer-surfactant system, in which amphiphilic cellulose acts as the polymeric component, while commercial oligomeric glycol-based frothers represent the surfactant counterpart. While the ecotoxicity of the studied commercial frother is minor, HPMC is a nontoxic and biodegradable molecule that can be produced from sustainable sources, i.e. plants and trees (Sannino et al., 2009).

The interest behind the use of polymer-surfactant (PS) mixtures stems from the positive results obtained in other industries where stabilization of foams is of interest, such as food, fuel, cosmetics, and pharmaceutical (Bureiko et al., 2015; Sannino et al., 2009; Wei et al., 2018). However, froth stabilization with PS-mixtures has not been explored in the field of mineral processing, to the best of the authors' knowledge. An additional reason why transition towards using chemicals such as HPMC may be of interest, is that it is already being produced on an industrial scale (Dickinson, 2003; Sannino et al., 2009). Although a detailed economic analysis of flotation using the proposed formulations is beyond the scope of this work, it can be mentioned that, according to prices available from wholesale traders, the cost of HPMC is comparable with molecules used as commercial frothers.

A vast amount of literature (Langevin, 2009; Nahringbauer, 1997; Guzmán et al., 2016), to name a few, discuss interactions of PS-mixtures in bulk solutions at high concentrations, which may affect bulk properties. However, it has also been reported that interactions at the air-liquid interface may occur in dilute solutions (Nikas and Blankschtein, 1994; Petkova et al., 2012; Taylor et al., 2007). Using dilute concentrations may be beneficial in terms of froth flotation, as such concentrations are not expected to affect bulk properties. Additionally, frother dosages are often close to their respective critical coalescence concentrations (CCC), which usually lie within the range of dozens of parts per million (Jávor, 2014; Wills and Finch, 2015).

According to the literature (Bain et al., 2010; Goddard and Anathapadmanabhan, 1993; Guzmán et al., 2016), the observed effects of PS-mixtures at the air-liquid interface can be either synergistic, antagonistic or non-interactive. The type of interaction has an effect on the properties of the interface, e.g., surface viscosity, surface elasticity, surface tension, film thickness and film stability (Fauser et al., 2015; Petkova et al., 2012; Schulze-Zachau and Braunschweig, 2017). Additionally, it has been claimed that, in the presence of surfactants, the adsorption behavior of polymers is linked to its capability of accessing trapped/non-equilibrium states (Bain et al., 2010). Indeed, the prospect of modifying interfacial properties, without affecting the bulk properties of the aqueous phase, by using dilute solutions of PS-mixtures is an interesting premise from the flotation point of view. Consequently, a major challenge is choosing a PS-mixture with properties specifically beneficial for flotation.

The PS-mixture chosen for this study consists of a non-ionic surfactant (DowFroth 200, in this study referred to as DF200) and a neutral amphiphilic polymer (HPMC). This system was carefully selected as its components are expected to have a weak interaction (Brackman, 1990), since strong interactions from oppositely charged molecules are documented to result in a reduced foamability, which may be detrimental to flotation (Petkova et al., 2012). On the other hand, the less intense interaction between non-ionic species is expected to offer a controlled increase in froth stability (Petkova et al., 2012). The hypothesis hereby posed is that the superior level of froth stability offered by PS-mixtures may be beneficial for the flotation process (Ahmed and Jameson, 1989; Ata, 2012).

This exploratory study consists, in the first place, on the characterization of two-phase (air and liquid) foams produced with aqueous solutions of the above-mentioned amphiphilic species and their 1:1 mixture. The study of foam stabilization properties includes dynamic surface tension (DST), bubble size, foam height and foam stability measurements. Secondly, a set of froth flotation experiments for the separation of a sphalerite model ore are presented, with the goal of evaluating:

i. the use of cellulose-based amphiphilic derivatives as frothers in the flotation of a sphalerite, using a commercial frother (DF200) as benchmark
ii. the differences in flotation performance with HPMC of two molecular sizes
iii. the limits of HPMC and its mixtures as flotation frothers

The choice of sphalerite as case-study mineral system is due to the economic relevance of Zn production. The current study is part of a larger research project whose aim is to thoroughly evaluate the possibility of using cellulose-based derivatives to support the introduction of green chemicals in mineral processing.

2. Materials and methods

2.1. Materials

The frothers used in this study were DF200, a commercial polyglycol ether-based frother, supplied by Nasaco International LLC and two different HPMC molecules supplied by Sigma-Aldrich (Product No. H8384 and 423238) (Fig. 1). The HPMC molecules are hereby referred to as HPMC 22k and HPMC 10k, referring to their average molecular weights according to their product specification. In addition, the supplier states that HPMC 22k has an average methoxyl content of 28−30% and an average hydroxypropyl content of 7−12%, while in the case of HPMC 10k these values are 29% and 7%, respectively.

Sodium ethylxanthate (SEX) was used as the collector and was obtained from TCI (Product No. E0195) with a purity of >95%. Copper Sulfate Pentahydrate ($CuSO_4 \cdot 5H_2O$) was used as activator and was purchased from VWR Chemicals Belgium (Catalog No. 23165.298) with a purity of >98%. Finally, pH was regulated using $Ca(OH)_2$ purchased from VWR Chemicals Belgium (Catalog No. 470300-588), with a purity of >98%.

The model ore consisted of a mixture of sphalerite and quartz. Sphalerite samples were ordered from Ward's Science (Catalog No. 470025-804), originating from Piedras Verdes, Chihuahua, Mexico, with an approximate Zn grade of 54% according to induced coupled plasma (ICP) analyses conducted in-house. The gangue mineral in the synthetic ore sample was quartz (SiO_2) provided by Sibelco Nordic Oy Ab. The declared nominal purity of the quartz was 99.2% and the nominal particle size was 0.1−0.6 mm. The mineralogy of these samples was further corroborated with XRD-analyses conducted in house. The results presented in the Supplementary Information (S1), confirm that both minerals are of high purity.

All chemicals and materials were used as received, without any further purification. Additionally, the water used in all aspects of the study was Pure Water (PW) with a resistivity of 15 MΩ cm and was generated with an Elga Purelab Option-R 7/15.

2.2. Methods

2.2.1. Bubble and foam properties

Bubble size measurements were run in a 10 l flotation column made from plexiglass®, manufactured in-house (Fig. 2).
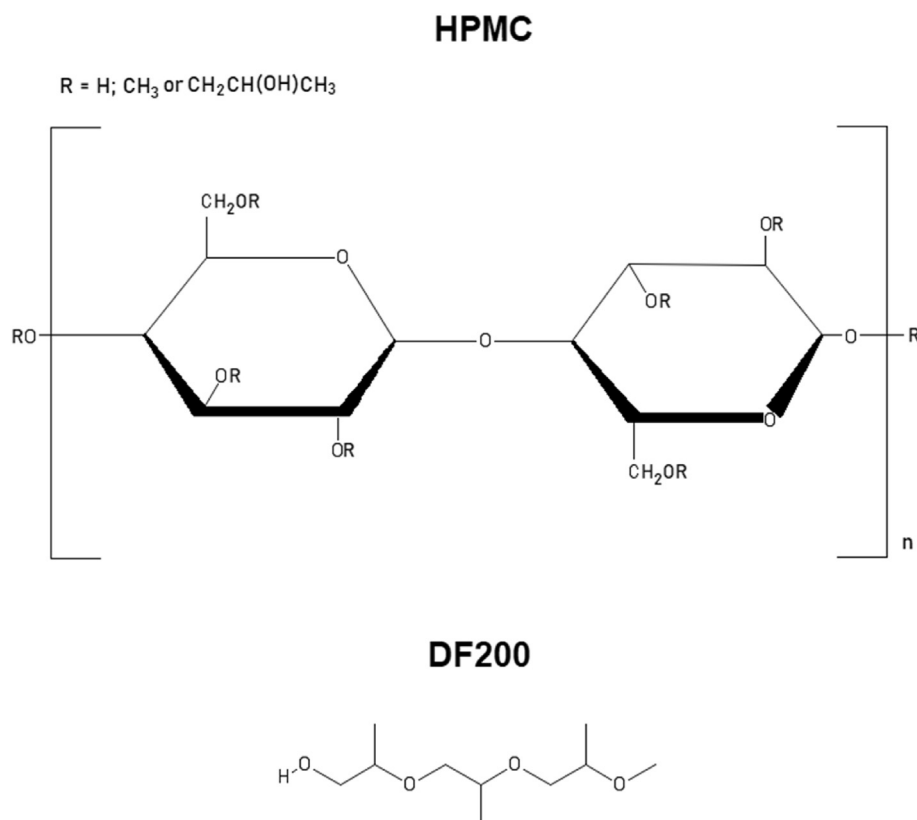
HPMC

R = H; CH$_3$ or CH$_2$CH(OH)CH$_3$

DF200

Fig. 1. Chemical structures of the studied frothers.

A more detailed description of the methodology can be found in Nuorivaara and Serna (2016). In short, the bubbles were formed by blowing air through a sparger with 5 μm openings and collecting the bubbles from the column to a bubble viewing chamber via a bubble collecting tube. Digital images were captured with a high-resolution digital camera through a glass window in the viewing chamber using red backlight. The images thus obtained were analyzed with a Matlab® image analysis routine to determine the minimum and maximum diameters (d_{min} and d_{max} respectively) of each bubble and consequently the equivalent diameter of each bubble according to Eq. (1) (Jávor et al., 2015)
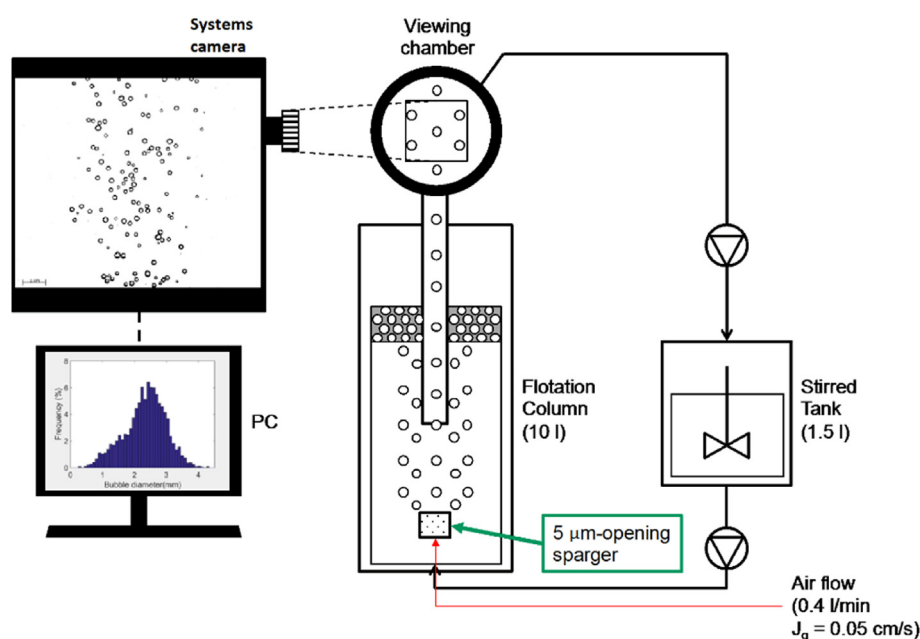

Fig. 2. Schematics of the bubble size measurement equipment.

$$d_{eq} = \sqrt[3]{d_{max}^2 d_{min}} \tag{1}$$

The bubble diameters from all bubbles in a single measurement were used to calculate the Sauter mean diameter (D_{32}) (Jávor et al., 2015) of the specific measurement as:

$$D_{32} = \frac{\sum d_{eq}^3}{\sum d_{eq}^2} \tag{2}$$

After each bubble size measurement, foam height and foam stability measurements were conducted in the same flotation column. Foam height was determined as the average of the highest and lowest points of the foam height around the column. The foam stability was determined as the time required by the foam to reach half of its original height after the air flow was turned off.

Foam stability measurements were performed under conditions resembling the subsequent flotation experiments, with pH stabilized at 11.1. The measurements were run in duplicates or triplicates. The complete set of experiments is presented in Table 1.

20 ml samples were taken from each bubble size measurement (Table 1) for DST measurements. The DST of the samples were analyzed with a BPA-800, according to the maximum bubble pressure method. The equipment was provided by Attension (former KSV-instruments).

2.2.2. Flotation experiments

The ore samples used for flotation experiments were a synthetic combination of the two mineral samples described in the Section 2.1, i.e., quartz and sphalerite. The sphalerite rocks were crushed in two stages: first, with a laboratory scale jaw crusher (Wedag MN 931/1 with a 200 × 125 mm gap and a minimum opening of 12 mm) and second, with a laboratory-scale roller crusher (Wedag) to a nominal particle size of <2.8 mm. The crushed sphalerite sample was divided into representative samples of approximately 90 g. The initial Zn concentration of the sphalerite sample was determined with an X-ray fluorescence (XRF) portable analyzer (X-Met 5100), and verified with induced coupled plasma (ICP) analysis. Meanwhile, quartz was divided into representative samples of approximately 510 g. Both groups of samples were prepared with a Retsch rotary sampling device and their masses were verified using a Precisa XB 6200D laboratory scale.

Due to differences in the hardness of the selected minerals, the samples were ground separately in order to obtain comparable particle sizes. The sphalerite samples were dry-ground in a ring mill (Fritsch Pulverisette 9) for 25 s, with tungsten carbide rings as grinding media, while the quartz sample was ground in a laboratory scale ball mill (Technical research center of Finland, type 14MK3/9), with a volume of 5.67 l. The grinding was conducted with a ball charge of 5.5 kg and with a 1:1 solid-to-water ratio for 50 min. The target d_{80} particle size for each mineral was of 90 μm, which was verified with laser diffraction particle size analysis

(Mastersizer 3000).

After comminution, the samples were combined in an Outokumpu 1.5 l laboratory scale flotation cell (presented in Fig. 3). The sphalerite samples were paired with quartz samples with a goal to match a target head grade of 8.1% as closely as possible. The total mass of model ore used in each flotation experiment was of ca. 600 g. For reference, the actual masses used in each flotation experiment can be found in the Supplementary Information (S2).

Before each flotation experiment, an initial wetting and conditioning procedure was conducted. First, the sample was stirred with an impeller speed of 1300 rpm for 5 min, after which the impeller speed was reduced to 900 rpm during addition of reagents. The conditioning procedure consisted of three consecutive additions of flotation reagents with a 3 min conditioning time in between. The sequence of reagents addition was i) activator ($CuSO_4$); ii) collector (SEX); and iii) frother (i.e., DF200, HPMC 22k, HPMC10k, Mix 22k or Mix 10k). In the case of frother mixtures, DF200 was added first and the respective HPMC (22k or 10k) immediately afterwards. After the final 3 min conditioning period, the impeller speed was increased to 1300 rpm and an air flow of 4 l/min (monitored with a rotameter) was turned on. This was regarded as the beginning of the flotation experiment (i.e., $\tau = 0$). The operating conditions for the flotation experiments are presented in Table 2.

The froth was collected into 4 different fractions based on flotation times: 0−3, 3−6, 6−10 and 10−14 min. For the first 10 min, the froth was scraped 10 times every 30 s and for 10−14 min 15 times every 60 s. Throughout the experiment, additional aqueous solution of frother at the target concentration was added to maintain the original pulp level.

After each flotation experiment, the collected froth fractions, as well as the final tailings, were dewatered, first by filtration and finally by heating overnight in a convection oven at 50 °C. The dry samples were subsequently weighted, and their elemental composition was analyzed by XRF. In addition, a selected group of samples were sent to ICP analysis. A linear regression model was used to correlate the XRF and the ICP data, which was consecutively applied as a correction factor to the rest of the XRF results. The use of two complementary analytical methods was performed since XRF is a quick measuring technique but analyzes elements only at the mineral surfaces. On the other hand, ICP analysis has a higher accuracy as the sample is dissolved into strong acid to determine the composition of the whole sample.

The accurate head grade of each experiment was determined after the flotation experiments by using mass balances based on the XRF results and the correction factor obtained from the ICP measurements. With this method, the average Zn grade of the feed was determined as 8.27 ± 0.26% with a 95% confidence. The exact head grade of each experiment was used when calculating the separation efficiencies (SE).

In order to properly study the goals mentioned in the Introduction, the experimental set up was divided into three different Campaigns. Each Campaign explored different pH and collector concentrations, as described in Table 3. As mentioned above, repetitions of selected experiments were carried out to determine the reproducibility of the experimental data (Supplementary Material, S3).

The different frother systems studied in each of Campaigns A-C were 1) DF200, 2) HPMC 22k 3) HPMC 10k 4) Mix 22k (DF200 + HPMC 22k as a 1:1 mixture) 5) Mix 10k (DF200 + HPMC 10k as a 1:1 mixture). In all cases, the total frother concentration was of 30 ppm (Table 2).

The flotation test results were studied in terms of mass pull, recovery, grade, SE and kinetics. SE was calculated according to Eq. (3) (Wills and Finch, 2015):

Table 1
Experimental conditions for bubble size, foam stability and dynamic surface tension measurements.

Frother system (repetitions)	Concentration (ppm)
DF200 (x3)	30
HPMC 22k (x3)	30
HPMC 10k (x2)	30
DF200 + HPMC 22k (x2)[a]	15 + 15
DF200 + HPMC 10k (x2)[b]	15 + 15

[a] Referred to as Mix 22k from hereon.
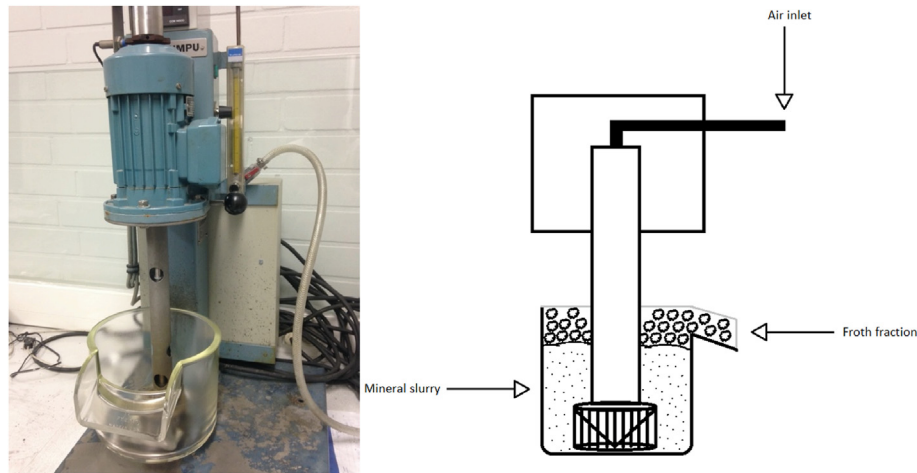[b] Referred to as Mix 10k from hereon.

Fig. 3. Picture and schematic of the Outokumpu 1.5 l flotation cell used in this study.

Table 2
Constant conditions of flotation experiments.

Parameter	Value
Air flow rate	4 l/min
Impeller speed	1300 rpm
Flotation time	14 min
Mass of solids	600 g
Solids content	33%
Total volume of suspension	1.5 l
Reagent	**Dose**
Activator	1565 g/t
Total frother concentration	30 ppm

Table 3
Experimental set up of the flotation experiments.

Campaign	pH	Collector (g/t)
A	11.1	80
B	12.3	80
C	12.3	20

$$SE = R_m - R_g = \frac{100 \, C \, m \, (c - f)}{(m - f) \, f} \qquad (3)$$

where SE is the separation efficiency, R_m is the % recovery of the valuable mineral, R_g is the % recovery of the gangue into the concentrate, C is the fraction of total feed weight that reports to the concentrate, f is the % of metal in the feed, c is the % of metal in the concentrate, and m is the % of metal content in the valuable mineral (for simplicity assumed to be exclusively ZnS in this study).

Additionally, the flotation kinetics were modelled following the first-order flotation rate (Wills and Finch, 2015):

$$R = R_{max}[1 - \exp(-k\tau)] \qquad (4)$$

where R is the total recovery at time (τ), R_{max} is the maximum theoretical recovery, k is the kinetic constant, and τ is time in seconds. The equation was solved by utilizing the Microsoft Excel™ solver application which iteratively determined values of k and R_{max} that best fit experimental data.

Finally, the experimental results for each frother system were analyzed with MODDE™ software to create a partial least squares (PLS) model for each frother system. The goal of the models was to

determine the sensitivity of each frother system towards changes in experimental conditions (i.e., collector concentration and pH). This could be achieved by comparing the values of the coefficients of each factor in the model. The model created by MODDE follows the form presented in Equation (5):

$$Y = C_0 + C_1 * C_{pH} + C_2 * C_{Col} + C_3 * C_{pH*pH} + C_4 * C_{Col*Col}$$
$$+ C_5 * C_{Col*pH} \qquad (5)$$

Where Y is the response (e.g. recovery or grade of the froth product), C_{0-5} are model coefficients, C_{pH} is the pH level and C_{Col} is the collector concentration. As seen, the model also considers a square response to the influence of pH and collector concentration, and their interaction.

3. Results and discussion

3.1. Effects on bubble and foam properties

3.1.1. Bubble coalescence prevention

The first property studied was the bubble size distribution of each frother system, presented in Fig. 4. As seen, at 30 ppm, DF200 and the PS-mixtures form a unimodal distribution of relatively small bubbles, whereas the distributions in the presence of pure HPMC are of bi-modal nature with HPMC 10k showing a larger spike of smaller bubbles. In previous works, a bi-modal bubble size distribution has been reported at concentrations lower than the corresponding critical coalescence concentration (CCC) of the frother, however transforming into unimodal as the frother concentration approaches its CCC (Finch et al., 2008; Jávor, 2014).

A further observation was that the bubble size distribution of HPMC remains bi-modal in concentrations exceeding its CCC (as seen in Supplementary Information, S4). This phenomenon reflects a different interfacial behavior of cellulose macromolecules compared with the regular frothers. With traditional frothers, bubble formation and coalescence prevention has been attributed to a combination of lower surface tension and electrostatic repulsion between molecules adsorbed at air-liquid interface. In the case of HPMC however, its large molecular size appears to offer an additional steric hindrance to coalescence. The exact nature of the coalescence prevention admittedly requires efforts beyond the scope of the current manuscript and will be the topic of a future work. Nevertheless, this coalescence prevention may be influential in the production of small bubbles with PS-mixtures since they do
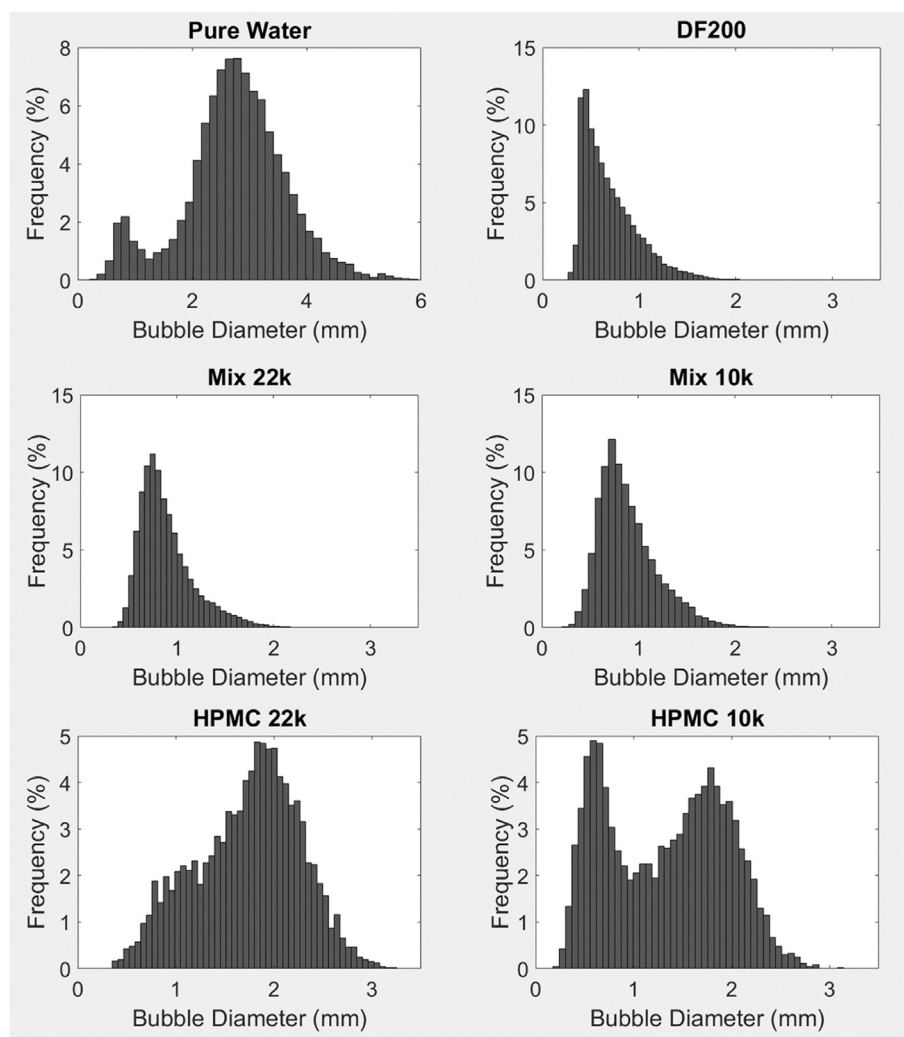
Fig. 4. Bubble size distributions of pure water and 30 ppm aqueous solutions of each studied frother system.

not impact surface tension in the same extent as DF200, as will be discussed in Section 3.1.3.

Based on the average D_{32} values in Table 4, the bubble size reducing properties of pure HPMC seem not as efficient as those of pure DF200 or the PS-mixtures. While this is partly a result of the inability of D_{32} to differentiate between monomodal or multimodal distributions, there is an undeniable presence of a significant

Table 4
D_{32} of studied frother systems with standard error in parentheses.

Frother	D_{32}
Water	3.26 (0.05)
DF200	1.02 (0.05)
HPMC 22k	2.01 (0.004)
HPMC 10k	1.81 (0.02)
Mix 22k	1.05 (0.04)
Mix 10k	1.04 (0.08)

Since small bubbles increase the total bubble surface area and consequently the probability of bubble-particle collisions (Wills and Finch, 2015), flotation in the presence of PS-mixtures can be expected to perform at least as well as DF200 based on their bubble size reduction properties.

population of large bubbles with HPMC. This could be attributed to a combination of slower adsorption kinetics of larger macromolecules such as HPMC (Nahringbauer, 1997) and a comparatively weaker surfactant behavior. Nevertheless, the population of smaller bubbles obtained with pure HPMC molecules could provide a flotation response that is worth exploring further. Indeed, combinations of small and large bubbles have been considered as advantageous by some authors (Tao, 2005) through a combination of better attachment of small bubbles and better levitation of larger bubbles.

3.1.2. Liquid film drainage prevention

As seen in Table 5, no stable foam was obtained in the presence of pure DF200, and thus, it was not possible to quantify foam height or its stability. It is likely that, in the case of DF200, the presence of hydrophobic solid particles is necessary to produce a stable froth phase with a measurable depth (Tan et al., 2010). On the other hand, both pure HPMC molecules and PS-mixtures were capable of forming a two-phase foam with a quantifiable stability. HPMC 22k had a more significant influence on the foam height in pure form than its 10k counterpart. Considering that the only significant difference between the two HPMC species hereby studied is their molecular weight, this suggests that foam formation is favored by the steric coalescence prevention offered by larger molecules (Hill

Table 5
Foam height and stability results.

Frother	Average Foam height (cm)	Foam stability (s)
DF200	0	0
HPMC 22k	2.35	60
HPMC 10k	1.7	20
Mix 22k	1.9	35
Mix 10k	2.35	40

and Eastoe, 2017; Pérez et al., 2006). There were no significant differences between PS-mixtures regarding foam collapsing time (i.e., stability). This implies that film drainage is similarly inhibited, and the rate defining condition is the use of PS-mixtures and not the molecular weight of the polymer fraction, at least with the systems hereby studied.

This phenomenon may be connected to an observation made by Schulze-Zachau and Braunschweigh (2017). In their corresponding PS-mixture, they found an optimal concentration ratio, which resulted in synergistic effects that were observed as maximum values of film thickness, foam stability and surface elasticity of interfaces. According to the definition of the surface dilatational modulus (Jávor, 2014), an increase in the surface elasticity also increases the viscoelasticity of the interface. Consequently, increased viscoelasticity has been connected to improved foam stability due to reduced drainage of liquid from the lamellae (Jávor et al., 2018; Wang et al., 2016) and is likely the mechanism behind the self-stabilizing effect observed in the presence of the PS-mixture hereby studied. Another aspect to consider in future studies is whether the optimal PS-mixture ratio in terms of surface elasticity is optimal in terms of flotation performance since the range for the optimal ratio in the study of Schulze-Zachau and Braunschweigh (2017) was relatively narrow and foam stability decreased significantly outside this range.

3.1.3. Interactions at the gas-liquid interface

According to Jávor et al. (2010), DF200 has fast adsorption kinetics and a relatively weak effect on the surface tension at the air-liquid interface at low concentrations. This is corroborated by the DST measurements in Fig. 5, where the decrease in surface tension in the presence of DF200 takes place within 2 s and then reaches a plateau at about 70.5 mN/m. On the other hand, long macromolecules are known to present comparatively slower adsorption kinetics, which is reflected in the behavior of HPMC presented in Fig. 5. As seen, the surface tension in the presence of both HPMC species has a less steep decay than DF200, and does not appear to reach stability after 12 s, set as maximum time for DST
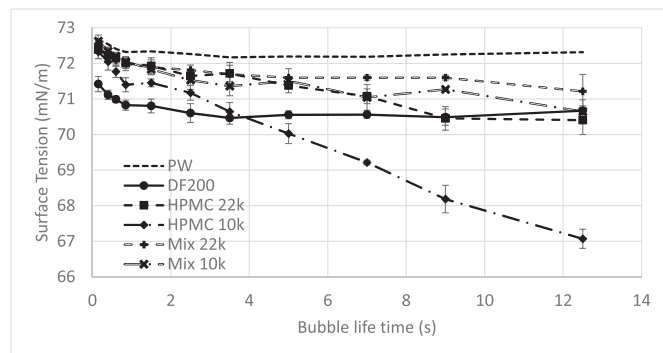

Fig. 5. Dynamic surface tension of the studied frother systems at total frother concentration of 30 ppm and a PW reference (error bars are represented with standard deviation).

measurements. Although slower, the final surface tension measured with both HPMC species is lower than that of the commercial frother, as is particularly observed in the case of HPMC 10k.

The dynamic surface tension of the 1:1 mixtures presents a behavior that resembles the relatively slower kinetics of pure HPMC, although with a higher value of surface tension at 12 s. The comparatively higher values of surface tension with PS-mixtures are indicative of the interaction of species, effectively inhibiting the adsorption of all existing amphiphilic segments at the air-liquid interface (Manousakis and Avranas, 2013). While at first glance this may seem like a negative effect, one should keep in mind that the film drainage prevention is a result of the polymer-surfactant interactions, as mentioned above. Indeed, Petkova et al. (2012) claimed that even weakly interacting systems are capable of increasing foaminess and foam stability, in agreement with the foam stability results presented in Section 3.1.2.

Furthermore, these results also corroborate previous claims that surface tension cannot be directly correlated to foamability or foam stability (Petkova et al., 2012; Pugh, 1996), requiring the characterization of other properties such as height and lifetime, as presented above.

3.2. Flotation experiments

As the unique foam stabilization characteristics of PS-mixtures have been identified, it is necessary to assess whether they translate into advantages in mineral froth flotation. The flotation results are presented for each individual Campaign (Table 6) with the goal to compare first the performance of each frother system within a certain set of operating conditions. Subsequently, the influence of operating conditions on the performance of the frother systems is analyzed, including its impact on recovery, grade, SE and flotation kinetics.

The standard deviation of selected experiments is presented between parenthesis in Table 6. The values show that the performance tendencies are within confidence limits, as the differences in measured values between frothers are in most cases larger than the standard deviation. Further analysis on the reproducibility of the experiments is presented in the Supplementary Information (S5).

### 3.2.1. Foam stabilization impact on flotation performance

When studying the results of Campaign A (Table 3, Fig. 6), a good performance by DF200 could be expected, since these operating conditions represent typical flotation environments in which this frother is used and, being a synthetic ore, the sphalerite particles are fully liberated. Comparatively, the flotation response was not as efficient in the presence of pure HPMC with recoveries of only 83 and 84%. Yet, when HPMC was mixed with DF200, the flotation performance was similar to that of the commercial frother in terms of recovery, grade and SE. In the case of Mix 22k, for example, a recovery of 98.65% was obtained with a slightly higher grade (44.81%) than that measured for DF200 (40.60%). The measured concentrate grades demonstrate, for the first time, that a suitable degree of selectivity can be achieved using PS-mixtures. Additionally, the maximum SE was obtained within a shorter flotation time (6 min) with PS-mixtures than with DF200 (10 min), reflecting comparatively faster kinetics.

When the pH was increased during Campaign B, a few additional trends were observed. Firstly, the flotation performance of pure DF200 declined significantly, compared to Campaign A. On the other hand, the performance of pure HPMC and PS-mixtures remained unaffected, or presented slight improvements. This observation was contradictory to the findings of Goryachev et al. (2015), who reported a reduced recovery of sphalerite when pH is increased to 12. It appears that the high tolerance towards changes

Table 6
Results of flotation experiments (Standard deviation in parentheses when available, based on data from Supplementary Information S5, Table S4).

Frother	Final Mass Pull	Final Recovery	Final Grade	Max SE	Time for Max SE (min)	k (s^{-1})
Campaign A						
DF200	19.21%	98.71%	40.60%	91.26%	10	0.0111
HPMC 22k	17.45%	83.24%	38.50%	75.83%	10	0.0067
HPMC 10k	16.55%	84.32%	40.99%	78.04%	6	0.0107
Mix 22k	17.09%	98.65%	44.81%	93.28%	6	0.0160
Mix 10k	17.94%	94.74%	41.48%	89.89%	6	0.0202
Campaign B						
DF200	14.21% (0.75%)	76.72% (2.97%)	45.90% (1.78%)	71.34% (2.74%)	14	0.0121 (0.0010)
HPMC 22k	15.93%	87.92%	43.13%	83.13%	6	0.0085
HPMC 10k	10.08%	81.75%	61.14%	80.74%	14	0.0098
Mix 22k	22.28%	96.37%	35.03%	91.10%	3	0.0204
Mix 10k	15.47%	98.81%	48.32%	96.48%	6	0.0186
Campaign C						
DF200	14.21% (4.24%)	56.38% (0.77%)	37.85% (7.08%)	49.89% (1.83%)	14	0.0103 (0.0004)
HPMC 22k	13.15%	69.41%	47.23%	64.92%	14	0.0056
HPMC 10k	11.03%	71.26%	52.91%	68.60%	14	0.0101
Mix 22k	26.83% (4.17%)	97.45% (2.01%)	31.96% (4.53%)	88.81% (1.96%)	6	0.0136 (0.0005)
Mix 10k	19.08%	98.68%	39.94%	91.75%	6	0.0146
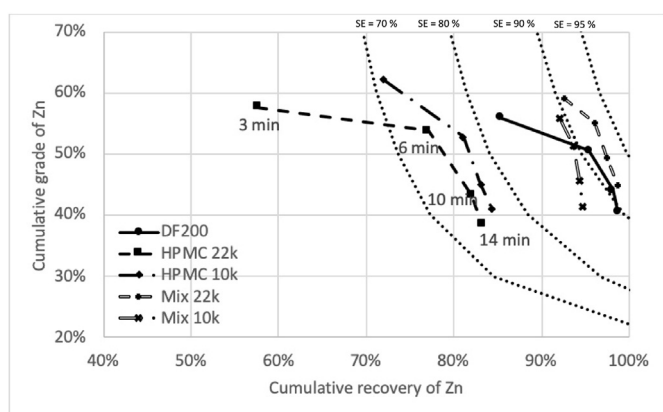
Fig. 6. Grade-recovery curves of Campaign A, all data points follow the same tendency of time fractions as exemplified for HPMC 22k (the dotted lines are visual references representing SE threshold values).
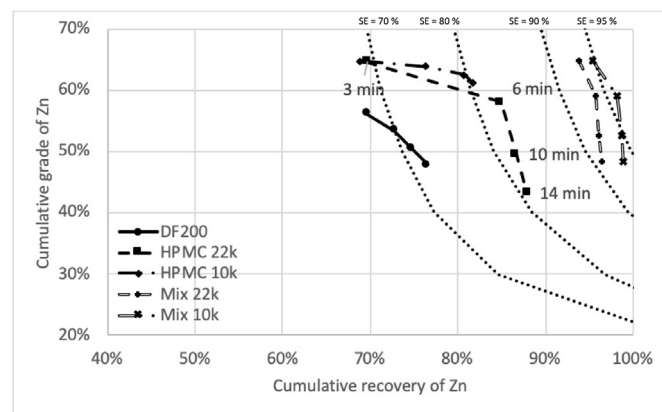
Fig. 7. Grade-recovery curves of Campaign B, all data points follow the same tendency of time fractions as exemplified for HPMC 22k (the dotted lines are visual references representing SE threshold values).

in pH reported with foams stabilized with HPMC (Coffey et al., 2006) also exists in flotation related phenomena. The authors theorize that such tolerance is maintained when HPMC is part of a PS-mixture. As a consequence, pure DF200 presented the worst SE of the studied frother systems under conditions of elevated pH (Fig. 7).

In Campaign C, the chemical environment was further modified by reducing the collector dosage to one quarter of its initial concentration. As seen in Fig. 8 and Table 6, the performance of DF200 continued to decline with reduced collector dosage. Similar observations were made by Celic (2015) who studied the effect of a less drastic reduction of xanthate collector concentration. The flotation performance with HPMC also declined with lower collector concentration. This may be an expected result, since collectors are responsible of the surface modification of minerals and thus are considered the main contributors to mineral recovery (Bulatovic, 2007). Albeit, in the presence of PS-mixtures, sphalerite recovery remained practically unaffected, with values of 96.03% and 98.68% in Campaign C. A first explanation may be related to the association between increased froth stability and improved recovery of valuables in a selective flotation process (Ata, 2012). In addition, this phenomenon can be connected to the unique ability
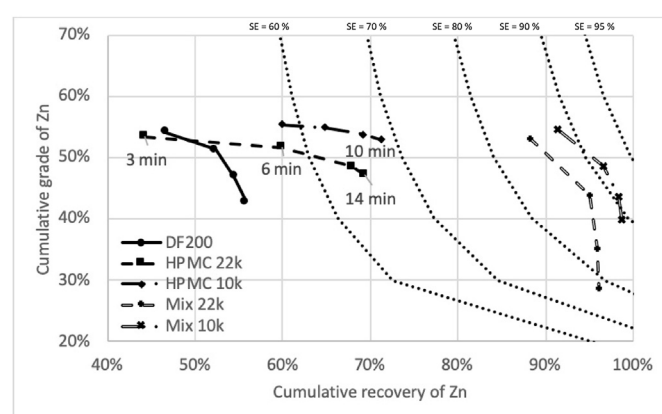
Fig. 8. Grade-recovery curves of Campaign C, all data points follow the same tendency of time fractions as exemplified for HPMC 22k (the dotted lines are visual references representing SE threshold values).

to produce self-stabilizing froths by PS-mixtures as mentioned in Section 3.1.2.

In all Campaigns, the maximum SE with the PS-mixtures was achieved within the first 6 min of the flotation experiment, being consistently shorter than the time necessary for maximum SE with the pure components (Table 6). This phenomenon is clearly observable in the grade-recovery dependencies of Campaigns A-C presented in Figs. 6-8. This finding reflects the faster kinetics obtained with PS-mixtures and seem justified considering that smaller bubble size and higher froth stability have been both connected to improved flotation kinetics (Ahmed and Jameson, 1989; Wills and Finch, 2015). As discussed in Section 3.1, the mixtures produced bubbles with smaller size compared to pure HPMC and a more stable foam compared to pure DF200 which indeed seems to manifest as improved flotation kinetics in a three-phase flotation system.

Admittedly, the use of model ores simplifies the flotation separation compared with natural ores as, e.g., the minerals are fully liberated and the composition is well known. Nevertheless, the tendencies observed in this manuscript are expected to be present also in natural ores, as the studied PS-mixture acts mainly on the properties of the air-liquid interface (Bain et al., 2010; Bulatovic, 2007). Studies on natural ores are a logical expansion on the present research and are planned for future publications.

3.2.2. Advantages of the robustness of PS-mixtures as frother systems

As mentioned above, the generation of froth with commercial polyglycol-based frothers such as DF200 is known to be highly dependent on the presence of sufficiently hydrophobic particles (Jávor, 2014). Consequently, it is highly sensitive to changes in the degree of hydrophobization of the mineral (Tan et al., 2010). On the other hand, PS-mixtures are able to sustain attributes beneficial to flotation on a wider scale of conditions, as they are able to produce stable foams even in two-phase (air-liquid) systems, as seen in the previous Sections discussing foam stability.

Especially, Mix 10k presented consistent results even when the conditions were significantly altered throughout all Campaigns, thus showing relatively small variations at a 95% confidence interval (Table 7). Considering that the flotation experiment results are sufficiently reproducible based on the standard deviation values in Table 6 (see details in Supplementary Material, S5), these results suggests that PS-mixtures are frother systems significantly more robust than pure polyglycol ether frothers, at least within the conditions studied in this manuscript.

This observation is further corroborated when the flotation results of each frother system are fit into independent PLS models, and their corresponding response coefficients for experimental variables (i.e., collector concentration and pH). The scaled-and-centered coefficient values corresponding to C_{1-5} of Equation (5) are presented in Fig. 9.

The value of the coefficient can be interpreted as the tolerance towards changes in pH and collector concentration within the studied conditions, with smaller coefficient values indicating a higher tolerance and vice-versa. Upon analysis of Fig. 9, it is evident that for all performance parameters, except kinetics, DF200 demonstrated the lowest overall tolerance towards changes in the studied conditions. HPMC was comparatively more tolerant, but the PS-mixtures represent the most robust systems studied, in particular Mix 10k.

Fig. 9 also indicates that in terms of flotation kinetics, the mixtures are more sensitive towards changes in chemical conditions. However, PS-mixtures consistently reported higher values of k (Table 6). Faster flotation was present with PS-mixtures even in Campaign C, where their kinetics were comparatively slower than in the other Campaigns. Therefore, it could be argued that the apparently higher sensitivity of flotation kinetics to operating conditions with PS-mixtures is a result of their comparatively higher values of kinetic constants.

Evidently, there are advantages from a consistent performance even under varying operating conditions. In the first place, the possibility to decrease the consumption of collectors can obviously translate into economic savings for the mineral processing operations. Secondly, the resilience to changes in pH for example, suggest that flotation performance will not be affected even under fluctuating conditions as a result of delays in process control response, for example. The operation at pH > 12 also opens the possibility to use conditions that favor the depression of mineral such as pyrite, commonly found in sphalerite mining sites.

4. Conclusions

This manuscript presents a first proof-of-concept on the use of amphiphilic cellulose derivatives as components of PS-mixtures in froth flotation. The experiments conducted in an ideal, fully liberated system revealed tendencies of remarkable potential for future advances in mineral processing if harnessed properly. Unlike what could be intuitively foreseen, the performance of the mixtures is not an average value of its pure frother counterparts. The stabilization mechanism in the presence of a weakly interacting PS-mixture is a combination of faster adsorption of the surfactant at the air-liquid interface combined with steric hindrance provided by the cellulose derivative. It was found that these two-phase phenomena result in properties beneficial for flotation. Indeed, the PS-mixtures consistently outperformed their pure components in most measured metrics during froth flotation of sphalerite, most importantly recovery, SE and kinetics. Additionally, the presence of the PS-mixture provided a robust flotation response even under significant variations of pH and collector concentration.

The most influential difference found between the commercial frother and the PS-mixtures was the latter's apparent independence from hydrophobic particles to stabilize the froth, which resulted in the increased robustness towards changes in operating conditions. Such improvements in efficiency and robustness of operation provided may also be attractive in the study of chemical systems or processing environments that were earlier deemed impractical due to unstable froth.

Finally, it is worth mentioning that, in order to further develop and understand this novel frother system, it is necessary to follow up with a systematic approach, progressing towards more complex mineralogies in model ore systems and ultimately testing the proposed chemical system with real ore under conditions that are closer to industrial practice.

Declaration of competing interest

The authors declare the following financial interests/personal relationships which may be considered as potential competing interests:

We wish to draw the attention of the Editor to the following

Table 7
Performance of Mix 10k in changing operating conditions (Campaigns A-C).

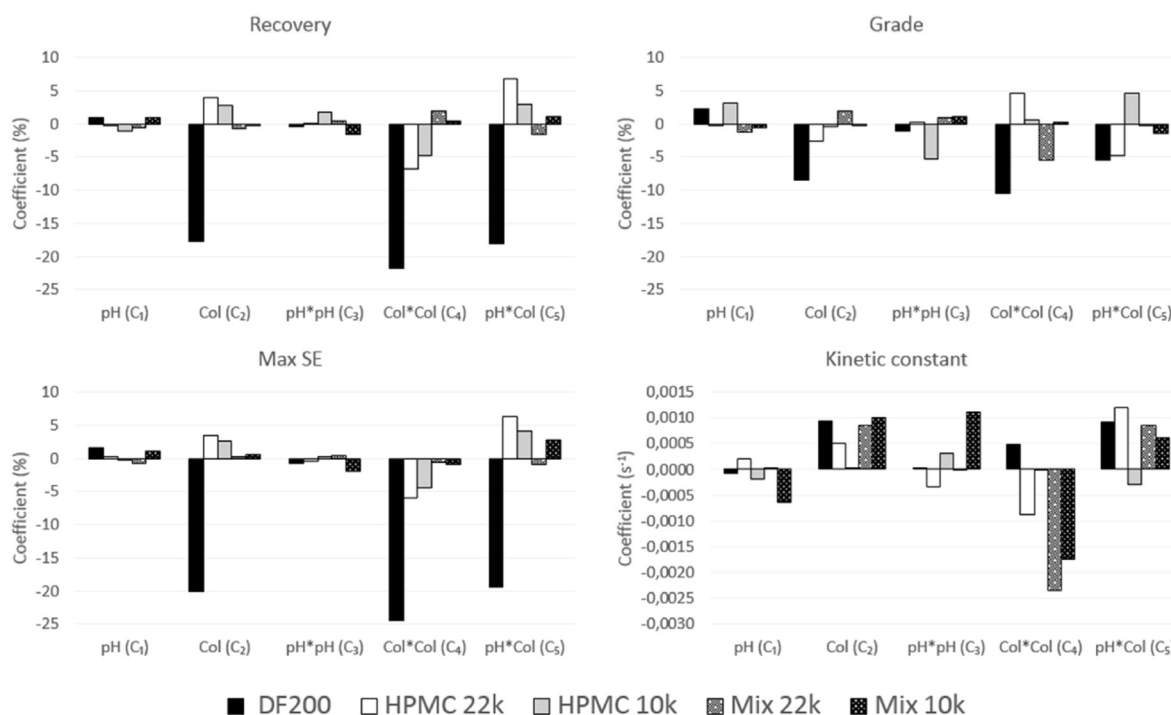| Campaign	Mass pull	Recovery	Grade	Max SE
A	17.94%	94.74%	41.48%	89.89
B	19.81%	99.06%	37.82%	96.48
C	19.08%	98.68%	39.94%	91.75
Mean	18.94%	97.49%	39.75%	92.71
Standard error	0.54%	1.38%	1.06%	1.96
95% CI	±2.34%	±5.95%	±4.58%	±8.44

Fig. 9. Coefficient values of each frother system for recovery, grade, maximum SE and kinetic constant.

facts which may be considered as potential conflicts of interest: some of the experimental results presented have been used to file a patent application (WO2019155116 (A1)).

We confirm that the manuscript has been read and approved by all named authors and that there are no other persons who satisfied the criteria for authorship but are not listed. We further confirm that the order of authors listed in the manuscript has been approved by all of us.

We confirm that we have given due consideration to the protection of intellectual property associated with this work and that there are no impediments to publication, including the timing of publication, with respect to intellectual property. In so doing we confirm that we have followed the regulations of our institutions concerning intellectual property.

We understand that the Corresponding Author is the sole contact for the Editorial process (including Editorial Manager and direct communications with the office). He/she is responsible for communicating with the other authors about progress, submissions of revisions and final approval of proofs. We confirm that we have provided a current, correct email address which is accessible by the Corresponding Author and which has been configured to accept email from: rodrigo.serna@aalto.fi.

CRediT authorship contribution statement

Ted Nuorivaara: Conceptualization, Investigation, Formal analysis, Writing - original draft. **Rodrigo Serna-Guerrero:** Methodology, Supervision, Writing - review & editing.

Acknowledgements

Appendix A. Supplementary data

Supplementary data to this article can be found online at https://doi.org/10.1016/j.jclepro.2020.121143.

References

Ahmed, N., Jameson, G.J., 1989. Flotation kinetics. Miner. Process. Ext. Met. Rev. 5, 77−99. https://doi.org/10.1080/08827508908952645.

Ata, S., 2012. Phenomena in the froth phase of Flotation − a review. Int. J. Miner. Process. 102−103, 1−12. https://doi.org/10.1016/j.minpro.2011.09.008.

Aznar-Sánchez, J.A., Velasco-Muñoz, J.F., Belmonte-Ureña, L.J., Manzano-Agugliaro, F., 2019. Innovation and technology for sustainable mining activity: a worldwide research assessment. J. Clean. Prod. 221, 38−54. https://doi.org/10.1016/j.jclepro.2019.02.243.

Bain, C.D., Claesson, P.M., Langevin, D., Meszaros, R., Nylander, T., Stubenrauch, C., Titmuss, S., von Klitzing, R., 2010. Complexes of surfactants with oppositely charged polymers at surfaces and in bulk. Adv. Colloid Interface Sci. 155 (1−2), 32−49. https://doi.org/10.1016/j.cis.2010.01.007.

Brackman, J., 1990. The Interaction between Water-Soluble Polymers and Surfactant Aggregates. Ph.D. thesis. University of Groningen, The Netherlands.

Bulatovic, S.M., 2007. Handbook of Flotation Reagents: Chemistry, Theory and Practice, first ed. Elsevier Science & Technology Books, Oxford, United Kingdom, p. 458.

Bureiko, A., Trybala, A., Kovalchuk, N., Starov, V., 2015. Current applications of foams formed from mixed surfactant-polymer solutions. Adv. Colloid Interface Sci. 222, 670−677. https://doi.org/10.1016/j.cis.2014.10.001.

Celic, I.B., 2015. Mineralogical interpretation of the collector dosage change on the sphalerite flotation performance. Int. J. Miner. Process. 135, 11−19. https://doi.org/10.1016/j.minpro.2014.12.003.

Coffey, D.G., Bell, D.A., Henderson, A., 2006. Cellulose and cellulose derivatives. In: Stephen, A.M., Philips, G.O., Williams, P.A. (Eds.), Food Polysaccharides and Their Applications, second ed. CRC Press, Boca Raton, pp. 147−179.

Dickinson, E., 2003. Hydrocolloids at interfaces and the influence on the properties of dispersed systems. Food Hydrocolloids 17 (1), 25−39.

Fauser, H., von Klitzing, R., Campbell, R.A., 2015. Surface adsorption of oppositely charged C_{14}TAB-PAMPS mixtures at the air/water interface and the impact on foam film stability. J. Phys. Chem. B 119 (1), 348−358. https://doi.org/10.1021/jp509631b.

Finch, J.A., Nesset, J.E., Acuña, C., 2008. Role of frother on bubble production and behavior in flotation. Miner. Eng. 21, 949−957. https://doi.org/10.1016/j.mineng.2008.04.006.

Goddard, E.D., Ananthapadmanabhan, K.P., 1993. Interactions of Surfactants with Polymers and Proteins. CRC Press, Boca Raton, pp. 123–277.

Goryachev, B.E., Kyaw, Z.Y., Nikolaev, A.A., Polyakova, Y.N., 2015. Perculiarities of sphalerite flotation by butyl potassium xanthate and sodium dithiophosphate in lime medium. Tsvetnye Met. 11 https://doi.org/10.17580/tsm.2015.11.02.

Guzmán, E., Llamas, S., Maestro, A., Fernández-Peña, L., Akanno, A., Miller, R., Ortega, F., Rubioa, R.G., 2016. Polymer-surfactant systems in bulk and at fluid interfaces. Adv. Colloid Interface Sci. 233, 38–64. https://doi.org/10.1016/j.cis.2015.11.001.

Hill, C., Eastoe, J., 2017. Foams: from nature to industry. Adv. Colloid Interface Sci. 247, 496–513. https://doi.org/10.1016/j.cis.2017.05.013.

Huang, Z., Cheng, C., Li, L., Guo, Z., He, G., Yu, X., Liu, R., Han, H., Deng, L., Fu, W., 2018. Morpholine-based gemini surfactant: synthesis and its application for reverse froth flotation of carnallite ore in potassium fertilizer production. J. Agric. Food Chem. 66 (50), 13126–13132. https://doi.org/10.1021/acs.jafc.8b05560.

Huang, Z., Cheng, C., Liu, Z., Zeng, H., Feng, B., Zhong, H., Luo, W., Hu, Y., Guo, Z., He, G., Fu, W., 2019. Utilization of a new Gemini surfactant as the collector for the reverse froth flotation of phosphate ore in sustainable production of phosphate fertilizer. J. Clean. Prod. 221, 108–112. https://doi.org/10.1016/j.jclepro.2019.02.251.

Jávor, Z., 2014. Frother Controlled Interfacial Phenomena in Dynamic Systems – a Holistic Approach. Ph.D. Dissertation. Aalto University. Department of Materials Science and Engineering.

Jávor, Z., Schreithofer, N., Heiskanen, K., 2010. Fast adsorption phenomena at air/liquid interfaces. In: XXV International Mineral Processing Congress, Brisbane, Australia, pp. 2015–2023.

Jávor, Z., Schreithofer, N., Heiskanen, K., 2015. Micro- and nano-scale phenomena effect on bubble size in mechanical flotation cell. Miner. Eng. 70, 109–118. https://doi.org/10.1016/j.mineng.2014.09.010.

Jávor, Z., Schreithofer, N., Heiskanen, K., 2018. Kernel functions to flotation bubble size distributions. Miner. Eng. 125, 200–205. https://doi.org/10.1016/j.mineng.2018.05.012.

Keijer, T., Bakker, V., Slootweg, C., 2019. Circular chemistry to enable a circular economy. Nat. Chem. 11, 190–195. https://doi.org/10.1038/s41557-019-0226-9.

Kinnunen, P.H., Kaksonen, A.H., 2019. Towards circular economy in mining: Opportunities and bottlenecks for tailings valorization. J. Clean. Prod. 228, 153–160. https://doi.org/10.1016/j.jclepro.2019.04.171.

Langevin, D., 2009. Complexation of oppositely charged polyelectrolytes and surfactants in aqueous solutions. A review. Adv. Colloid Interface Sci. 147–148, 170–177. https://doi.org/10.1016/j.cis.2008.08.013.

Manousakis, M., Avranas, A., 2013. Dynamic surface tension studies of mixtures of hydroxypropylmethylcellulose with the double chain cationic surfactants didodecyldimethylammonium bromide and ditetradecyldimethylammonium bromide. J. Colloid Interface Sci. 402, 237–245. https://doi.org/10.1016/j.jcis.2013.03.064.

Nagaraj, D.R., Farinato, R.S., 2016. Evolution of flotation chemistry and chemicals: a century of innovations and the lingering challenges. Miner. Eng. 96–97, 2–14. https://doi.org/10.1016/j.mineng.2016.06.019.

Nahringbauer, I., 1997. Polymer-surfactant interaction as revealed by the time dependance of surface tension. The EHEC/SDS/water system. Langmuir 13, 2242–2249. https://doi.org/10.1021/la960976i.

Nikas, Y.J., Blankschtein, D., 1994. Complexation of nonionic polymers and surfactants in dilute aqueous solutions. Langmuir 10, 3412–3528. https://doi.org/10.1021/la00022a026.

Nuorivaara, T., Serna-Guerrero, R., 2016. In: A Study on the Properties of Foams Produced with Cellulose-Based Molecules with an Outlook on Flotation, Proceedings of the International Minerals Processing Congress, Quebec, Canada, Sept 11-15.

Pérez, O.E., Carrera-Sánchez, C., Rodríguez-Patino, J.M., Pilosof, A.M.R., 2006. Thermodynamic and dynamic characteristics of hydroxypropylmethylcellulose adsorbed films at the air-water interface. Biomacromolecules 7, 388–393. https://doi.org/10.1021/bm050757o.

Petkova, R., Tcholakova, S., Denkov, N.D., 2012. Foaming and foam stability for mixed polymer-surfactant solutions: effect of surfactant type and polymer charge. Langmuir 28, 4996–5009. https://doi.org/10.1021/la3003096.

Peçanha, R.E., da Fonseca de Albuquerque, M.D., Antoun Simão, R., de Salles Leal Filho, L., de Mello Monte, M.B., 2019. Interaction forces between colloidal starch and quartz and hematite particles in mineral flotation. Colloids Surf., A 562, 79–85. https://doi.org/10.1016/j.colsurfa.2018.11.026.

Pugh, R.J., 1996. Foaming, foam films, antifoaming and defoaming. Adv. Colloid Interface Sci. 64, 67–142. https://doi.org/10.1016/0001-8686(95)00280-4.

Sannino, A., Demitri, C., Madaghiele, M., 2009. Biodegradable cellulose-based hydrogels: design and applications. Materials 2, 353–373. https://doi.org/10.3390/ma2020353.

Schulze-Zachau, F., Braunschweig, B., 2017. Structure of polystyrenesulfonate/surfactant mixtures at air-water interfaces and their role as building blocks for macroscopic foam. Langmuir 33, 3499–3508. https://doi.org/10.1021/acs.langmuir.7b00400.

Stahel, W.R., 2016. The circular economy. Nature 435–438. https://doi.org/10.1038/531435a.

Tan, S.N., Yang, Y., Horn, R.G., 2010. Thinning of a vertical free-draining aqueous film incorporating colloidal particles. Langmuir 26, 63–73. https://doi.org/10.1021/la9021118.

Tao, D., 2005. Role of bubble size in flotation of coarse and fine particles – a review. Separ. Sci. Technol. 39 (4), 741–760. https://doi.org/10.1081/SS-120028444.

Taylor, D.J.F., Thomas, R.K., Penfold, J., 2007. Polymer/surfactant interactions at the air/water interface. Adv. Colloid Interface Sci. 132, 69–110. https://doi.org/10.1016/j.cis.2007.01.002.

van Schalkwyk, R.F., Reuter, M.A., Gutzmer, J., Stelter, M., 2018. Challenges of digitalizing the circular economy: assessment of the state-of-the-art of metallurgical carrier metal platform for lead and its associated technology elements. J. Clean. Prod. 186, 585–601. https://doi.org/10.1016/j.jclepro.2018.03.111.

Velázquez Martínez, O., Van Den Boogaart, K.G., Lundström, M., Santasalo-Aarnio, A., Reuter, M., Serna-Guerrero, R., 2019. Statistical entropy analysis as tool for circular economy: proof of concept by optimizing a lithium-ion battery waste sieving system. J. Clean. Prod. 212, 1568–1579. https://doi.org/10.1016/j.jclepro.2018.12.137.

Wang, J., Nguyen, A.V., Farrokhpay, S., 2016. A critical review of the growth, drainage and collapse of foams. Adv. Colloid Interface Sci. 228, 55–70. https://doi.org/10.1016/j.cis.2015.11.009.

Wei, B., Li, H., Li, Q., Lu, L., Li, Y., Pu, W., Wen, Y., 2018. Investigation of synergism between surface-grafted nano-cellulose and surfactants in stabilized foam injection process. Fuel 211, 223–232. https://doi.org/10.1016/j.fuel.2017.09.054.

Wills, B.A., Finch, J.A., 2015. Wills' Mineral Processing Technology: an Introduction to the Practical Aspects of Ore Treatment and Mineral Recovery. Butterworth-Heinemann.